Supporting Information for

"Linking host traits, interactions with competitors, and disease: Mechanistic foundations for disease dilution"

Alexander T. Strauss[1,2] (straussa@umn.edu), Anna M. Bowling[1] (bowlinan@indiana.edu), Meghan A. Duffy[3] (duffymeg@umich.edu), Carla E. Cáceres[4] (cecacere@illinois.edu), and Spencer R. Hall[1] (sprhall@indiana.edu)

[1]Department of Biology, Indiana University, Bloomington, IN 47401, USA

[2]Present address: Department of Ecology, Evolution, and Behavior, University of Minnesota, St. Paul, MN 55108, USA

[3]Department of Ecology and Evolutionary Biology, University of Michigan, Ann Arbor, MI 48109, USA

[4]School of Integrative Biology, University of Illinois at Urbana-Champaign, Urbana, IL 61801, USA

Corresponding author information: Alex Strauss; straussa@umn.edu

Appendix S1: Supplemental Methods and Results

In this Appendix, we provide additional methodological details for our trait measurement assays and mesocosm experiment. Then, we display time series for each focal host genotype in the mesocosm experiment. First, G2 and G8 serve as illustrative examples across the range of trait space (Fig. S1). Then, we present G1, G3, and G4 (Fig. S2), and finally G5, G6, and G7 (Fig. S3). Next, we provide two additional analyses. First, for each link between a focal host trait and mesocosm variable, we compare results of linear GLS models with linear mixed models. We summarize the differences in Table S1. Second, we test whether epidemic size correlates more strongly with focal host density during week 2 (when spores were added), rather than mean focal host density throughout the experiment. We show these results in Figure S4. Finally, we provide details of the path models. First, we summarize the fit statistics used to judge both models (Table S2). Then, we report the parameters of path models featured in Fig. 4 (Table S3) and Fig. 5 (Table S4).

Trait Measurement Assays

We quantified indices of two important traits, susceptibility and competitive ability, for eight different focal host genotypes. All genotypes were chosen from existing laboratory cultures that had been isolated from lakes in southwestern Michigan or southwestern Indiana (USA). Using limited prior knowledge of these genotypes, we selected focal host genotypes with the aim of spreading the range of both traits. Prior to trait measurement assays, all genotypes were grown in isoclonal cultures and fed high quality, laboratory-cultured algae (2.0 mg mass/L/day *Ankistrodesmus falcatus*). Cultures were maintained in high-hardness COMBO (artificial lake

water media) under ideal conditions for three generations, in order to standardize any maternal effects.

Susceptibility: We calculated an index of susceptibility (the transmission coefficient, β) from infection assays. The transmission coefficient represents the probability of a focal host becoming infected, given the density of infectious spores (Z), the duration of spore exposure (t), and body length of the focal host (L). Susceptibility depends on body length because larger hosts encounter parasites at a higher rate due to faster foraging (Hall *et al.* 2007). For the assay, we first reared cohorts of neonates of each isoclonal line (fed 1.0 mg mass/L/day of highly edible algal food, *Ankistrodesmus*). After 5 days, individuals were isolated in 15 mL of media. Fifteen of these individuals were exposed to each of three densities of fungal spores (Z): 75, 200, or 393 spores/mL. Spores (< 6 weeks old) were all reared in a standard focal host genotype. After ~8 hours of exposure time (t), we measured body length of all individuals (L) with a dissecting microscope and micrometer. Thereafter, we transferred each individual to a fresh 50 mL tube of media daily, until death. Dead individuals were visually inspected with the dissecting microscope to diagnose infection. Individuals that died too early to determine infection were omitted from the analysis. This assay was conducted in three different experimental blocks. Two isoclonal lines were repeated among blocks to control for any block effects resulting from variation in spore infectivity.

To estimate susceptibility (β) from this transmission assay, we simplified a previously used mathematical model (Hall *et al.* 2007; Hall *et al.* 2012). This model assumes that initial density of susceptible hosts in the assay (S_i; one per tube) decreases as susceptible hosts (S) contact spores (Z) at rate βL^2, where β is size-controlled susceptibility, and L^2 is proportional to host surface area. Specifically, $\frac{dS}{dt} = -\beta L^2 S Z$. Solving this equation for the final density of

susceptible hosts (S_f), after exposure time (t), yields: $S_f = S_i \exp(-\beta L^2 Z t)$. We estimated susceptibility (β) for each isoclonal line, using maximum likelihood and the BBLME package in R (Bolker 2008; R Core Team 2017). The binomial distribution (infected or not) served as the likelihood function. After controlling for block effects, we bootstrapped standard errors for each focal host genotype.

Competitive Ability: We calculated an index of competitive ability with juvenile growth rate assays on low resources (as in Hall *et al.* 2012). Mass accrual of neonates during a 5–6 day juvenile period is directly proportional to adult fitness (Lampert & Trubetskova 1996). In turn, competitive ability depends on fitness when resources are limiting (reviewed in Grover 1997). Thus, focal hosts with high juvenile growth rates on low food resources should be strong competitors.

To calculate juvenile growth rate, we first isolated cohorts of neonates (< 24 hours old) for each focal host genotype. We obtained initial day 0 mass measurements (m_i), by drying and weighing 6–13 neonates (mean N = 11.1 per genotype) with a Mettler microbalance (Mettler-Toledo, Columbus, Ohio, USA). We also placed 11–18 live neonates (mean N = 14.5 per genotype) in separate 50 mL tubes of media. Each day, we transferred these individuals into fresh media (fed 0.15 mg mass/L *Ankistrodesmus* daily). Then, after 5 or 6 days (d), we dried and weighed these individuals, yielding final mass estimates (m_f). With these data, we calculated juvenile growth rate on low resources (GR) as the mean for each combination of initial and final mass estimates: $GR = [\ln(m_f) - \ln(m_i)] \,/\, d$. Finally, we bootstrapped standard errors around means for each focal host genotype in R.

Mesocosm Methods and Time Series

Each replicate of the mesocosm experiment was housed in a 75-L acid-washed polyethylene tank in a climate-controlled room and grown under a 16 L: 8 D light cycle. We filled tanks to 60 L with high-hardness COMBO (artificial lake water) and added initial doses of nitrogen (300 ug L-1 N as $NaNO_3$) and phosphorus (20 ug L-1 P as K_2HPO_4). Then we inoculated all tanks with algae (50 mg dry weight *Ankistrodesmus falcatus*). Throughout the experiment, we replaced evaporated COMBO and replenished nutrients, assuming a 5% exponential daily loss rate.

Focal host genotypes drove divergent outcomes in the mesocosm experiment (Figs. S1, S2 & S3). Two genotypes (G2 & G8) qualitatively illustrate a range of outcomes (Fig. S1). G2 featured low susceptibility and competitive ability (see Fig. 1). In the mesocosms with G2, epidemics remained small. The density of competitor/diluters increased throughout the experiment, and competition lowered focal host density, especially during weeks 3–8 (Fig. S1a). Both the density and prevalence of infected hosts remained low but were still reduced by diluters (Fig. S1 b & c, respectively). In contrast, G8 featured higher susceptibility and competitive ability (see Fig. 1). G8 fueled larger epidemics and competed relatively strongly. The density of competitor/diluters remained low, and competition (on average) did not depress focal host density as strongly (Fig. S1d). Both the density and prevalence of infected hosts were higher and more clearly reduced by diluters (Fig. S1 e & f, respectively). Mesocosm dynamics of the other six genotypes fell largely within this range. However, the impacts of diluters on infection prevalence proved inconsistent (see Figs. S2 & S3). Mean mesocosm responses off all eight genotypes are synthesized with linear (Figs. 2–3) and path models (Figs. 4–5) in the main text.

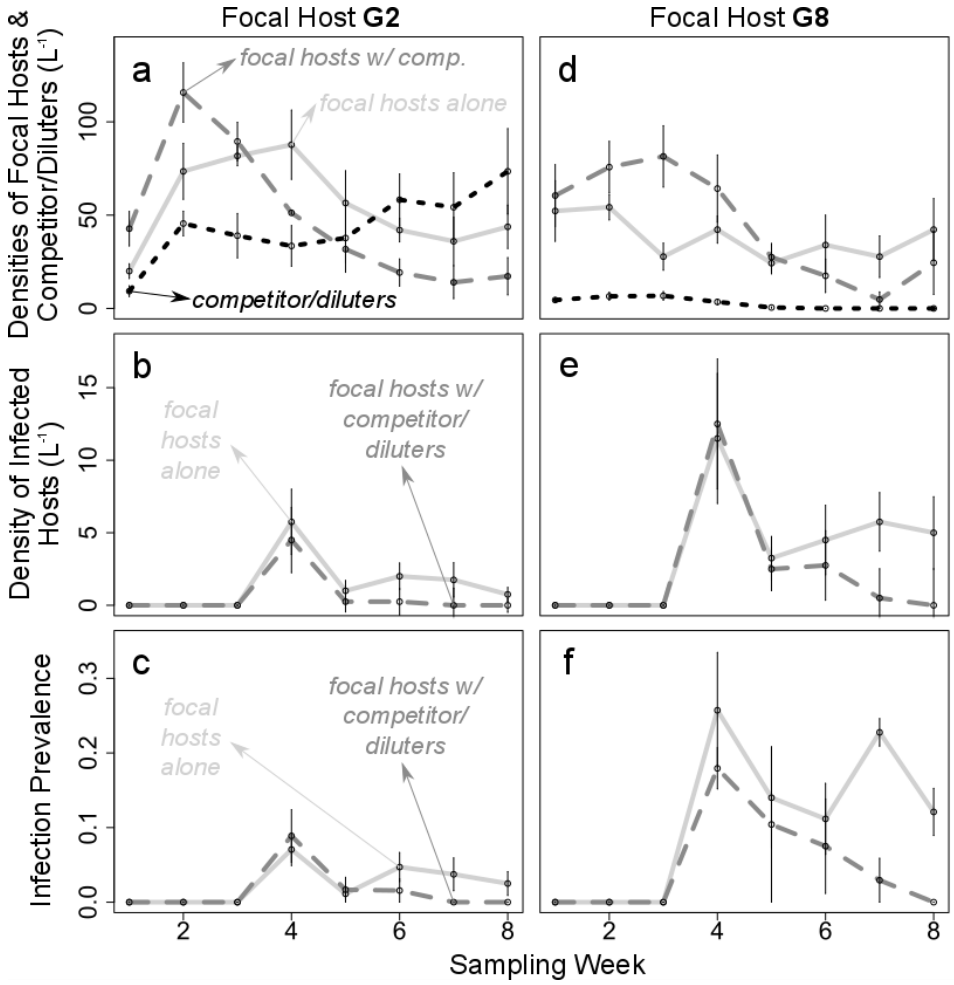

Figure S1. *Mesocosm dynamics of two illustrative focal host genotypes varying in key traits.* Time series show changes in host and diluter densities (top), the density of infected hosts (center), and infection prevalence (bottom), for two focal host genotypes (columns). **a – c)** Focal host G2 (named "Bristol 111") features low indices of susceptibility and competitive ability (see Fig. 1). a) It competes weakly and maintains a low b) density and c) prevalence of infected hosts. **d – f)** In contrast, focal host G8 (named "Midland 273") features high indices of susceptibility and competitive ability. d) It competes more strongly and maintains a higher e) density and f) prevalence of infected hosts. b, c, e & f) Competitor/diluters reduce both metrics of disease for both genotypes. Error bars are standard errors. Key: solid lines = focal hosts alone; dashed = focal hosts in competition; dotted = competitor/diluters in competition.

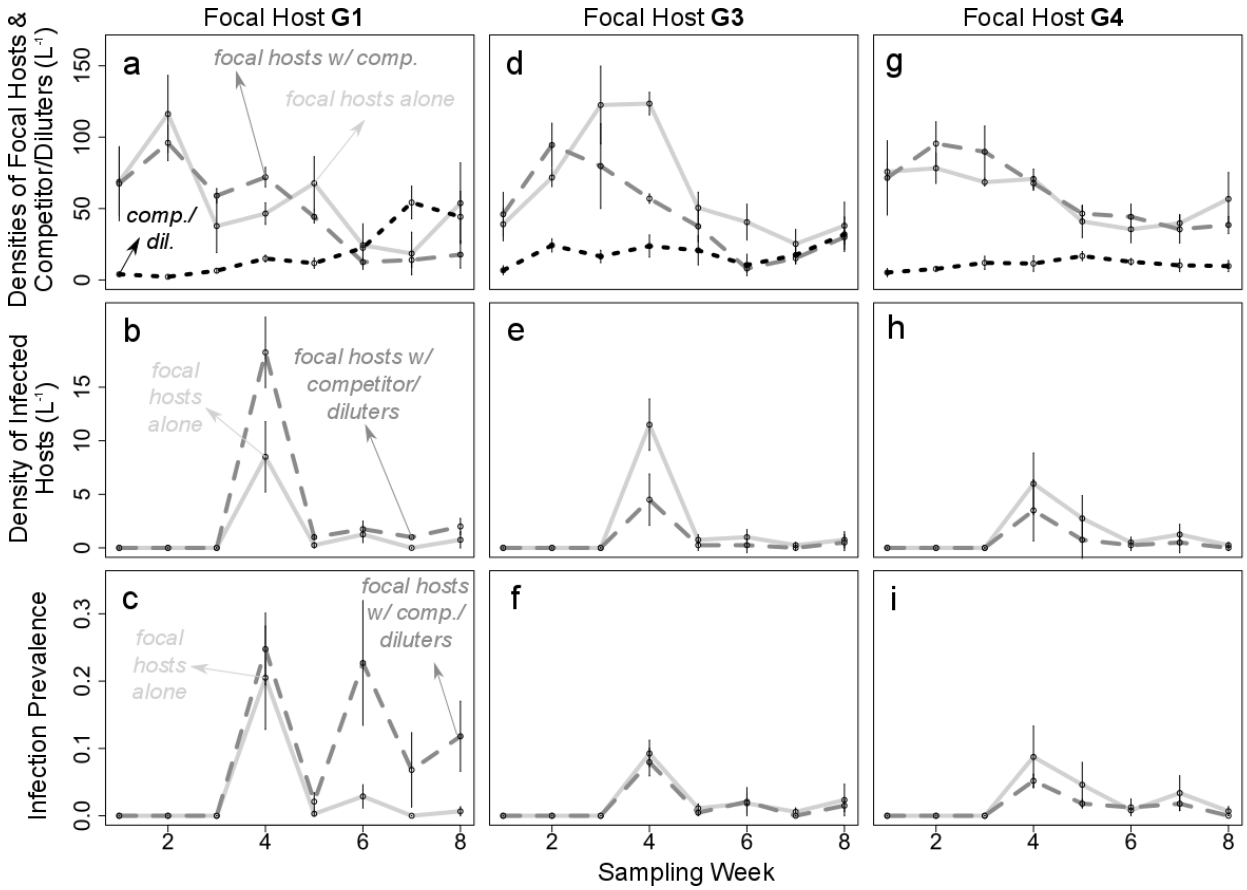

Figure S2. *Mesocosm dynamics of three focal host genotypes varying in key traits.* Time series show changes in host densities (top), the density of infected hosts (center), and infection prevalence (bottom), for three focal host genotypes (columns). Focal host G1 (left column; named "Downing 282") a) competed weakly and maintained a moderate b) density and c) prevalence of infections. Focal host G3 (center column; named "Bristol 10") d) competed moderately, and maintained a low e) density and f) prevalence of infections. Focal host G4 (right column; named "Warner 5") g) competed strongly, but also maintained a low h) density and i) prevalence of infections. Competitor/diluters had various impacts on both metrics of disease (see Figs. 2–5 for quantitative synthesis). Error bars are standard errors. Solid lines = focal hosts alone; dashed = focal hosts in competition; dotted = competitor/diluters in competition.

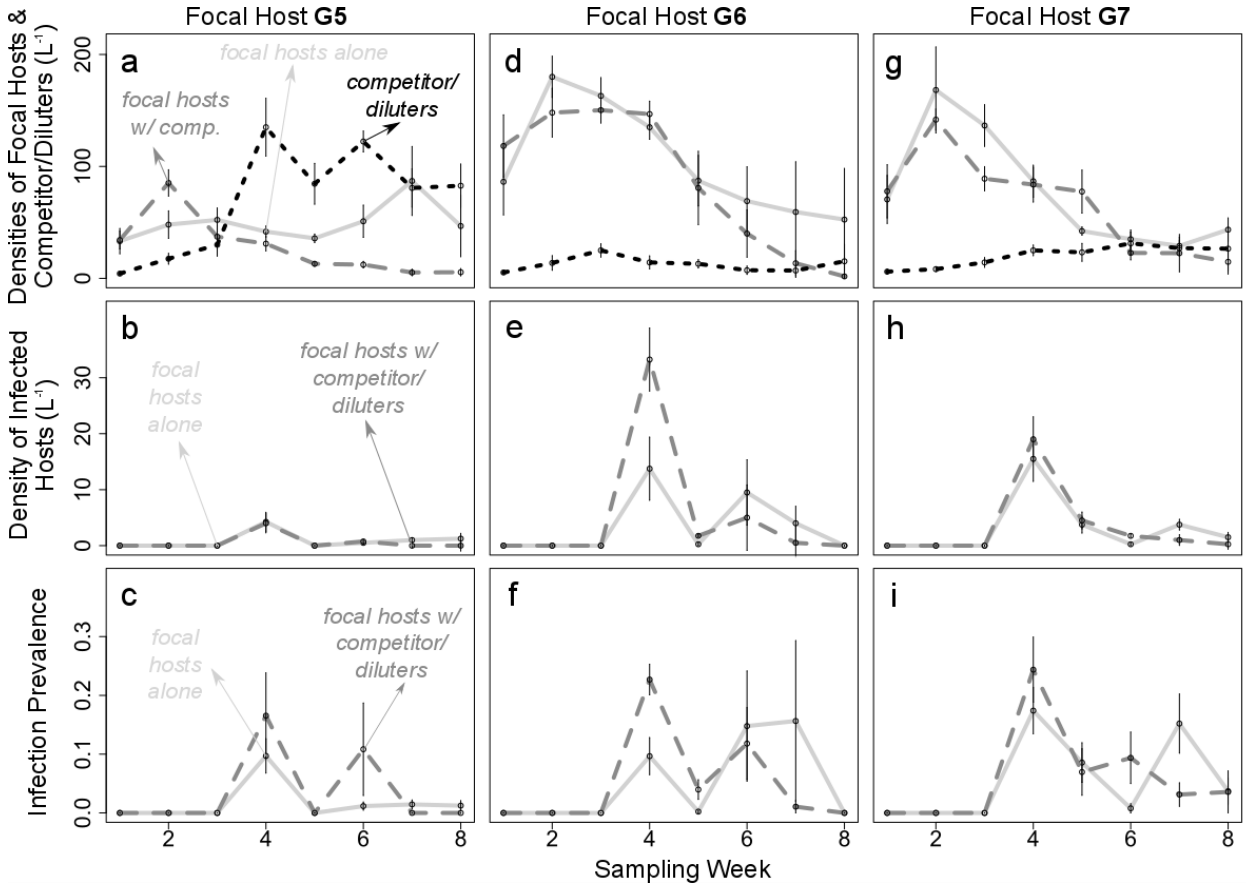

Figure S3. *Mesocosm dynamics of three focal host genotypes varying in key traits.* Time series show changes in host densities (top), infection prevalence (center), and the density of infected hosts (bottom), for three focal host genotypes (columns). Focal host G5 (left column; named "Bristol 112") a) competed weakly and maintained a low b) density and c) prevalence of infections. Focal host G6 (center column; named "Midland 263") d) competed moderately and maintained a moderate e) density and f) prevalence of infections. Focal host G7 (right column; named "Dogwood 4") g) competed strongly and maintained a moderate h) density and i) prevalence of infections. Competitor/diluters had various impacts on both metrics of disease (see Figs. 2–5 for quantitative synthesis). Error bars are standard errors. Solid lines = focal hosts alone; dashed = focal hosts in competition; dotted = competitor/diluters in competition.

Simple Linear vs. Linear Mixed Models

Our goal is to predict variation in epidemic size with and without diluters from focal host traits. Therefore, we manipulated focal host traits by selecting different genotypes, and traits serve as the independent variable in several of our analyses (Figs. 2 & 3a). However, some degree of measurement error likely impacted our trait assays. Hence, an alternative statistical approach could also include focal host genotype as a random effect in these models. Incorporating this mixed model structure (random intercept only) tended to raise *P* values relative to *P* values in the corresponding GLS models. One of three significant relationships remained significant, and the remaining two became trends ($P < 0.1$; Table S1).

Table S1. *Comparisons between GLS and mixed models.*

Focal Host Trait	**Covariate**	**Independent Variable**	**Figure Panel**	**Linear Model Results**	**Mixed Model Results**
Suscep-tibility (β)	Pres./Abs. of Competitor/ Diluters (*C*)	Density of Infected Hosts	2a	$\boldsymbol{\beta}$**:** $\boldsymbol{P = 0.0046}$ *C*: $P = 0.79$ $\beta \times C$: $P = 0.71$	β: $P = 0.096$ *C*: $P = 0.75$ $\beta \times C$: $P = 0.65$
Suscep-tibility (β)	Pres./Abs. of Competitor/ Diluters (*C*)	Infection Prevalence	2b	$\boldsymbol{\beta}$**:** $\boldsymbol{P = 0.008}$ *C*: $P = 0.24$ $\beta \times C$: $P = 0.21$	$\boldsymbol{\beta}$**:** $\boldsymbol{P = 0.043}$ *C*: $P = 0.18$ $\beta \times C$: $P = 0.16$
Competitive Ability	None	Density of Comp./Dil.	3a	$\boldsymbol{P < 0.0001}$	$P = 0.098$

Focal Host Density During Week 2:

In the analyses presented in the main text, higher mean focal host density elevated the mean density of infected hosts ($P = 0.0048$; Fig. 3d), but did not impact mean infection prevalence ($P = 0.58$; Fig. 3f). This decoupling between host density and infection prevalence may seem surprising. To evaluate the robustness of this result, we tested whether focal host density during week 2 (when parasite spores were added) might impact mean infection prevalence more clearly. However, week 2 focal host density was strongly correlated with mean focal host density ($P < 0.0001$; Fig. S4a). In this model, presence of competitor/diluters also lowered mean focal host density ($P = 0.0024$). Because week 2 density and mean density were highly correlated, the impacts of each density metric on disease were qualitatively similar. Higher week 2 densities of focal hosts still elevated mean densities of infected hosts ($P = 0.028$; Fig. S4b). Similarly, mean infection prevalence was still not impacted by week 2 density of focal hosts ($P = 0.97$; Fig. S4c). Presence of competitor/diluters was not a significant covariate predicting either the density ($P = 0.67$) or prevalence of infections ($P = 0.96$). Thus, the decoupling of host density and infection prevalence remains robust.

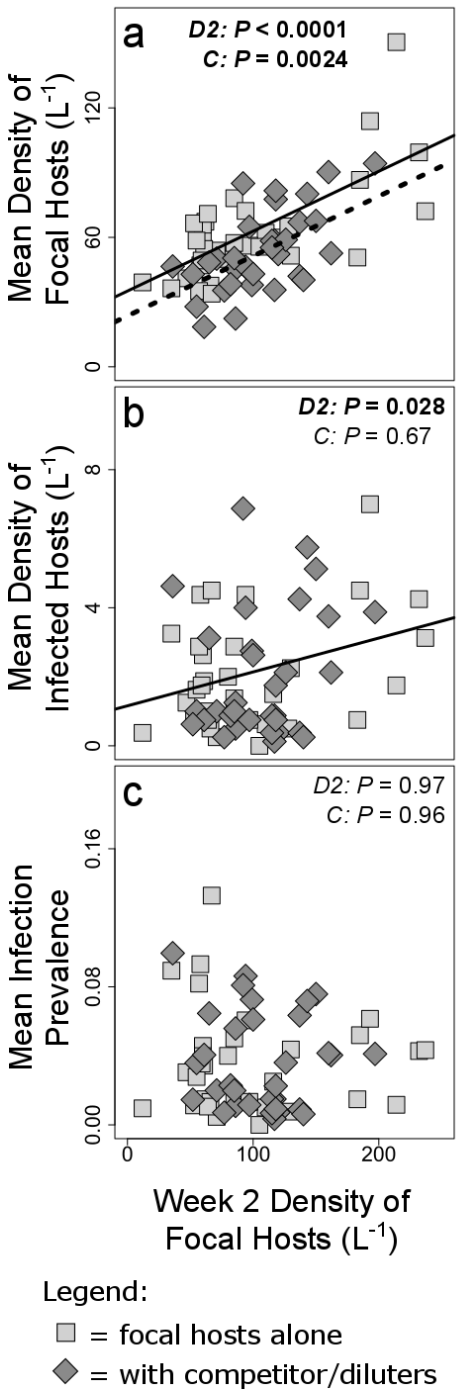

Figure S4. *Density of focal hosts during week 2 (when parasites were added) correlates with mean focal host density and impacts disease metrics accordingly.* a) Higher focal host density during week 2 correlates with higher mean focal host density throughout the experiment. Hence, impacts of week 2 density on disease mirror impacts of mean focal host density. Specifically, b) it elevates mean density of infected hosts, but c) does not impact mean infection prevalence. *P* values are results of linear models. Key: *D2* = focal host density during week 2 [solid lines]; *C* = presence of competitor/diluters; squares = focal hosts alone; diamonds = with competitor/diluters.

Table S2. *Test statistics, cutoff criteria for determining good model fit, and statistics of both path models*. Test statistics exceeding the desired cutoff criteria confirm that the hypothesized model is a relatively good fit for the observed data (Hu and Bentler 1999).

Test Statistic	**Desired Cutoff**	**Fig. 4**	**Fig. 5**
Robust Satorra-Bentler Chi Square	*P* value > 0.05	*P* = 0.637 **df* = 2	*P* = 0.654 **df* = 1
Robust Comparative Fit Index (CFI)	CFI > 0.95	1.000	1.000
Robust Tucker Lewis Index (TLI)	TLI > 0.95	1.576	2.083
Root Mean Square Error of Approximation (RMSEA)	RMSEA < 0.06	0.000 †(0.000:0.104)	0.000 †(0.000:0.000)
Standardized Root Mean Square Residual (SRMR)	SRMR < 0.08	0.035	0.035

Key to abbreviations: **df* = degrees of freedom; † = 90% confidence interval

Table S3. *Parameters for the path model in Fig. 4*. Bold lines indicate significance.

*Dep. Var./ Component	Explanatory Variable	*Par. Est.	*SE	Z-value (Wald)	*P* Value	*Stand. Par. Est.
Density of	**Susceptibility, *β***	**0.408**	**0.142**	**2.878**	**0.005**	**0.411**
Inf. Hosts ~	**Dens. Competitor/Diluters**	**-0.162**	**0.059**	**-2.759**	**0.006**	**-0.164**
Density of	**Growth Rate Low Res.**	**-0.314**	**0.129**	**-2.431**	**0.015**	**-0.318**
Comp./Dil.~						
Modeled	Susceptibility, *β* ~~	58.14	39.20	1.483	0.138	0.583
Covariance:	Growth Rate Low Res.					
Intercepts:	Density of Infected Hosts	1.373	4.454	0.758	0.758	0.140
	Dens. Competitor/Diluters	36.15	12.40	2.914	0.004	3.631
	Susceptibility, *β*	28.08	3.772	7.443	0.000	2.835
	Growth Rate Low Res.	95.25	3.836	24.83	0.000	9.459
Variances:	Density of Infected Hosts	75.34	25.72	2.929	0.003	0.779
	Dens. Competitor/Diluters	89.11	47.27	1.885	0.059	0.899
	Susceptibility, *β*	98.05	30.86	3.177	0.001	1.000
	Growth Rate Low Res.	101.4	39.27	2.582	0.010	1.000

*Key to abbreviations: Dep. Var. = dependent variable; Par. Est. = parameter estimate; SE: = Standard error; Stand. = standardized

Table S4. *Parameters for the path model in Fig. 5.* Bold lines indicate significance.

*Dep. Var./ Component	Explanatory Variable	*Par. Est.	*SE	Z-value (Wald)	*P* Value	*Stand. Par. Est.
Density of	**Density of Focal Hosts**	**0.314**	**0.086**	**3.653**	**0.000**	**0.322**
Inf. Hosts ~	Dens. Competitor/Diluters	-0.049	0.054	-0.898	0.369	-0.050
	Susceptibility, β	**0.372**	**0.128**	**2.899**	**0.004**	**0.380**
Density of	**Dens. Competitor/Diluters**	**-0.379**	**0.123**	**-3.073**	**0.002**	**-0.380**
Focal Hosts ~						
Modeled	Susceptibility, β ~~	-15.89	13.71	-1.159	0.246	-0.161
Covariances:	Dens. Competitor/Diluters					
Intercepts:	Density of Infected Hosts	-6.575	5.312	-1.238	0.216	-0.679
	Density of Focal Hosts	28.73	2.864	10.03	0.000	2.894
	Dens. Competitor/Diluters	6.213	1.930	3.220	0.001	0.624
	Susceptibility, β	28.08	3.772	7.443	0.000	2.835
Variances:	Density of Infected Hosts	67.16	20.11	3.34	0.001	0.716
	Density of Focal Hosts	84.33	42.71	1.974	0.048	0.856
	Dens. Competitor/Diluters	99.12	53.76	1.844	0.065	1.000
	Susceptibility, β	98.05	30.86	3.177	0.001	1.000

*Key to abbreviations: Dep. Var. = dependent variable; Par. Est. = parameter estimate; SE: = Standard error; Stand. = standardized.

REFERENCES

Bolker, B.M. (2008) *Ecological Models and Data in R*. Princeton University Press.

Grover, J.P. (1997) *Resource Competition*. Chapman & Hall.

Hall, S.R., Becker, C.R., Duffy, M.A. & Caceres, C.E. (2012) A power-efficiency trade-off in resource use alters epidemiological relationships. *Ecology*, **93,** 645-656.

Hall, S.R., Sivars-Becker, L., Becker, C., Duffy, M.A., Tessier, A.J. & Cáceres, C.E. (2007) Eating yourself sick: transmission of disease as a function of foraging ecology. *Ecology Letters*, **10,** 207-218.

Lampert, W. & Trubetskova, I. (1996) Juvenile growth rate as a measure of fitness in *Daphnia*. *Functional Ecology*, **10,** 631-635.

R Core Team (2017) R: A language and environment for statistical computing. R Foundation for Statistical Computing, Vienna, Austria.